A Unified Passivity-based Control Framework for Position, Torque and Impedance Control of Flexible Joint Robots

Alin Albu-Schäffer, Christian Ott and Gerd Hirzinger

The International Journal of Robotics Research 2007; 26; 23
DOI: 10.1177/0278364907073776

Alin Albu-Schäffer
Christian Ott
Gerd Hirzinger

Institute of Robotics and Mechatronics
German Aerospace Center (DLR), Germany
Alin.Albu-Schaeffer@dlr.de
Christian.Ott@dlr.de
Gerd.Hirzinger@dlr.de

A Unified Passivity-based Control Framework for Position, Torque and Impedance Control of Flexible Joint Robots

Abstract

This paper describes a general passivity-based framework for the control of flexible joint robots. Recent results on torque, position, as well as impedance control of flexible joint robots are summarized, and the relations between the individual contributions are highlighted. It is shown that an inner torque feedback loop can be incorporated into a passivity-based analysis by interpreting torque feedback in terms of shaping of the motor inertia. This result, which implicitly was already included in earlier work on torque and position control, can also be used for the design of impedance controllers. For impedance control, furthermore, potential energy shaping is of special interest. It is shown how, based only on the motor angles, a potential function can be designed which simultaneously incorporates gravity compensation and a desired Cartesian stiffness relation for the link angles. All the presented controllers were experimentally evaluated on DLR lightweight robots and their performance and robustness shown with respect to uncertain model parameters. Experimental results with position controllers as well as an impact experiment are presented briefly, and an overview of several applications is given in which the controllers have been applied.

KEY WORDS—flexible joint robots, torque feedback, passivity-based control, impedance control, active vibration damping

The International Journal of Robotics Research
Vol. 26, No. 1, January 2007, pp. 23-39
DOI: 10.1177/0278364907073776

Figures appear in color online: http://ijr.sagepub.com

1. Introduction

The currently growing research interest in application fields such as service robotics, health care, space robotics, or force feedback systems has led to an increasing demand for light robot arms with a load to weight ratio comparable to that of human arms. These manipulators should be able to perform compliant manipulation in contact with an unknown environment and guarantee the safety of humans interacting with them. A major problem specific to the implementation of lightweight robot concepts is the inherent flexibility introduced into the robot joints. Consequently, the success in the above mentioned robotics fields is strongly dependent on the design and implementation of adequate control strategies which can:

- compensate for the weakly damped elasticity in the robot joints in order to achieve high performance motion control,
- provide the desired Cartesian compliant behavior of the manipulator,
- enable robust and fast manipulation in contact with unknown passive environments,
- provide safety and dependability in interaction with humans.

It is commonly recognized that these control goals require sensing capabilities that exceed the classical position measurement of industrial robots. The solution chosen in the case of the DLR lightweight robots (Figure 1) was to provide the

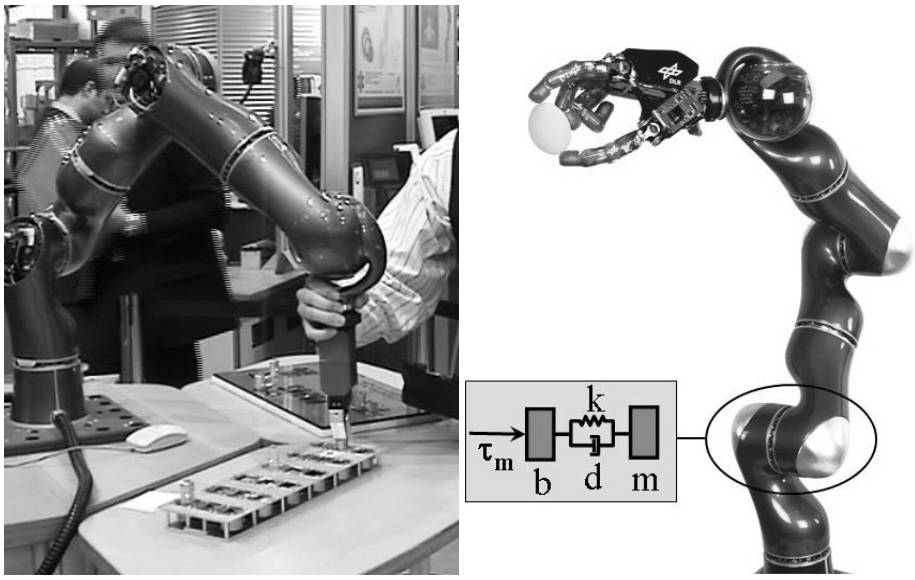

Fig. 1. The third generation of DLR lightweight robots, LWRIII. Left: teaching a peg in hole application at the Automatica robotic fair. Right: LWRIII with the DLR hand holding an egg. A schematic representation of one flexible joint is added.

joints with torque sensors in addition to motor position sensors (Hirzinger et al. 2001). The joint torque sensors play an essential role both for active vibration damping during free motion and for compliance and safe interaction control. Additionally, a 6 dof force–torque sensor was mounted on the robot wrist. The position control problem for flexible joint robots has been treated extensively in the robot control literature (Spong 1987; Tomei 1991; Brogliato et al. 1995; De Luca 2000; Lin and Goldenberg 1995). However, the problem of compliant motion control for interaction with unknown environments and with humans has been addressed only recently during consideration of robot flexibility (Goldsmith et al. 1999; Zollo et al. 2005; Ott et al. 2004; Albu-Schäffer et al. 2004b). The relevance of the topics becomes clear when looking at the latest hardware developments, where elasticity is deliberately introduced into the joints in order to increase the interaction performance and safety of robots (Morita et al. 1999; Zinn et al. 2004; Bicchi et al. 2003).

Due to the fact that the model structure is more complex than for rigid robots, there was still a gap between theoretical solutions (which often require very accurate models and the measurement or estimation of high order derivatives of the joint position) and the practical solutions commonly chosen for dealing with joint elasticity, which are not always based on firm theoretical background. Of course, the control literature for flexible joint robots contains various different possible approaches, especially to the position control problem. The best performance is theoretically given by decoupling-based approaches, which provide a partially or even fully linearized closed loop system and ensure global asymptotic stability also for the tracking case (Spong 1987; Brogliato et al. 1995; Lin and Goldenberg 1995; De Luca and Lucibello 1998; Lozano et al. 2000; Ott et al. 2002). These controllers, however, require as a state vector the link side positions up to their third derivative and/or a very accurate robot model. For the DLR robots these approaches resulted in only moderate performance and robustness. The situation with backstepping-based controllers is similar to that of decoupling-based approaches. On the other hand, singular perturbation-based controllers are easy to implement, but their performance is theoretically and practically limited to the case of relatively high joint stiffness. In order to cope with parameter uncertainty, adaptive extensions have been proposed for most controller types (Spong 1989; Nicosia and Tomei 1992; Lin and Goldenberg 1995; Spong 1995, Brogliato et al. 1995; Zhu and De Schutter 1999; Yim 2001; Ott et al. 2002), but even those methods are usually sensitive to unmodeled dynamics. For the DLR lightweight robots, we preferred the passivity-based approach described below, because it is based only on the available motor position and joint torque signals, as well as their first-order derivatives, and provides a high degree of robustness to unmodeled robot dynamics and in the contact with unknown environments. The developed framework is both theoretically sound and practically feasible, as demonstrated by the various applications realized so far using these controllers. The work most closely related to this paper can be traced back to Takegaki and Arimoto (1981) for the rigid robot case and contains, among others (Tomei 1991; Kelly 1997; Kelly and Santibanez 1998; Ortega et al. 1995; Lozano et al. 2000; Zollo et al. 2005). The main contributions of the

present work are the embedding of torque feedback into the passivity-based control approach, leading to a full state feedback controller[1], as well as the online gravity compensation approach which removes any lower bound restrictions on the position feedback gains. Together with the physical interpretation of the torque feedback as inertia scaling, this makes it possible to extend the concept from position control to joint and Cartesian impedance control.

In this paper we first describe the robot model and give an overview of the controller structures for the DLR robots in Section 2, present the position controllers and sketch the passivity based theoretical framework on which the controllers are based in Section 3, and go into some detail with the Cartesian impedance controller in Section 4. Finally we provide experimental data in Section 5 in order to exemplify the controller performance of both position and impedance control, and shortly describe some typical applications in Section 6.

2. Problem Statement and Framework Overview

2.1. Flexible Joint Model

In order to include the effects of joint elasticity, a one dof joint can be modelled by two inertias b and m which correspond to the rotor and to the link respectively, and which are interconnected by a spring-damper system with spring and damping constants k and d (Figure 1). Therefore each joint becomes a fourth-order system with the state given by, for example, the position and velocity of both rotor and link. In this way, for the entire robot, the following model structure based on Spong (1987) is assumed:

$$\boldsymbol{M}(\boldsymbol{q})\ddot{\boldsymbol{q}} + \boldsymbol{C}(\boldsymbol{q},\dot{\boldsymbol{q}})\dot{\boldsymbol{q}} + \boldsymbol{g}(\boldsymbol{q}) = \boldsymbol{\tau} + \boldsymbol{D}\boldsymbol{K}^{-1}\dot{\boldsymbol{\tau}} + \boldsymbol{\tau}_{\text{ext}} \quad (1)$$

$$\boldsymbol{B}\ddot{\boldsymbol{\theta}} + \boldsymbol{\tau} + \boldsymbol{D}\boldsymbol{K}^{-1}\dot{\boldsymbol{\tau}} = \boldsymbol{\tau}_m - \boldsymbol{\tau}_f \quad (2)$$

$$\boldsymbol{\tau} = \boldsymbol{K}(\boldsymbol{\theta} - \boldsymbol{q}) \quad (3)$$

The vectors $\boldsymbol{q} \in \mathbb{R}^n$ and $\boldsymbol{\theta} \in \mathbb{R}^n$ contain the link and motor side positions, respectively. The first equation contains, on the left-hand side, the well known rigid body dynamics with $\boldsymbol{M}(\boldsymbol{q}) \in \mathbb{R}^{n\times n}$, $\boldsymbol{C}(\boldsymbol{q},\dot{\boldsymbol{q}})\dot{\boldsymbol{q}}$, and $\boldsymbol{g}(\boldsymbol{q}) \in \mathbb{R}^n$ being the inertia matrix, the centripetal and Coriolis vector, and the gravity vector. In contrast to the rigid case, on the right-hand side one has the torque from the spring-damper system, denoted also by $\boldsymbol{\tau}_a$ later on in the paper $\boldsymbol{\tau}_a = \boldsymbol{\tau} + \boldsymbol{D}\boldsymbol{K}^{-1}\dot{\boldsymbol{\tau}} = \boldsymbol{K}(\boldsymbol{\theta}-\boldsymbol{q}) + \boldsymbol{D}(\dot{\boldsymbol{\theta}}-\dot{\boldsymbol{q}})$. The vector $\boldsymbol{\tau} \in \mathbb{R}^n$ represents the spring torques as defined by (3) and $\boldsymbol{\tau}_{\text{ext}} \in \mathbb{R}^n$ are the external torques acting on the robot. $\boldsymbol{K} = \text{diag}(k_i) \in \mathbb{R}^{n\times n}$ is the diagonal, positive definite joint stiffness matrix, and $\boldsymbol{D} = \text{diag}(d_i) \in \mathbb{R}^{n\times n}$ is the diagonal positive semi-definite joint damping matrix. The spring-damper torque is related to the motor torque $\boldsymbol{\tau}_m \in \mathbb{R}^n$ through another second-order equation (2), involving the diagonal, positive definite motor inertia matrix $\boldsymbol{B} = \text{diag}(b_i) \in \mathbb{R}^{n\times n}$.

1. In the references cited above, only motor position feedback is considered.

The vector $\boldsymbol{\tau}_f \in \mathbb{R}^n$ consists of the friction torques. The analysis in this paper focuses on the effects of joint flexibility and therefore $\boldsymbol{\tau}_f$ will be neglected in the following. In practice it is of course important to add also a friction compensation part to the controller in order to reduce the remaining friction to a minimum (torque feedback already reduces the friction effect considerably, as will become clear in Section 3.2). For the DLR robots, we use a model-based friction compensation (Albu-Schaffer 2001) and/or a motor disturbance observer. The state vector $(\boldsymbol{\theta}, \dot{\boldsymbol{\theta}}, \boldsymbol{\tau}, \dot{\boldsymbol{\tau}})$ used for control throughout the paper contains the motor positions $\boldsymbol{\theta}$ and the joint torques $\boldsymbol{\tau}$, both directly measured by sensors, as well as their first derivatives $\dot{\boldsymbol{\theta}}$ and $\dot{\boldsymbol{\tau}}$, which are computed numerically. Of course, in the absence of a torque sensor, the link side position $\boldsymbol{q}$ and its derivative $\dot{\boldsymbol{q}}$ can be used instead[2], leading to the state vector $(\boldsymbol{\theta}, \dot{\boldsymbol{\theta}}, \boldsymbol{q}, \dot{\boldsymbol{q}})$ which is linearly related to the previous one trough (3).

2.2. Framework Overview

The purpose of this paper is to introduce a novel control design and analysis framework, which allows the realization of various control structures known from the rigid robot case (such as position, force, impedance control) in the presence of significant elasticity in the joints. The viability and robustness of the methods for a large range of applications is thereby a major requirement. The framework is constructed from a passivity control perspective, by giving a simple and intuitive physical interpretation in terms of energy shaping to the feedback of the different state vector components.

- A physical interpretation of the joint torque feedback loop is given as the shaping of the motor inertia.
- The feedback of the motor position can be regarded as shaping of potential energy.

These interpretations enable a new view of a linear state feedback controller with gravity compensation as introduced in Section 3.1 and enables a generalization in several directions. First, it allows the extension to variable control gains, as described in Section 3.4, in order to increase control performance. Moreover, it allows the implementation of impedance control in Cartesian coordinates (Section 4), by changing only the nature of the desired (shaped) potential energy through the motor position feedback and expressing it in Cartesian coordinates, as done in the rigid robot case. The torque loop can be independently designed in this case (as well as in the joint impedance control case) for maximal performance in terms of reducing motor inertia and friction. For all proposed controllers, a Lyapunov stability analysis can be done easily using storage functions from the passivity representation as candidate Lyapunov functions. In order to preserve passivity, the

2. However, an accurate value of the torque is crucial for controller performance and its estimation through (3) can be unsatisfactory in the presence of small offsets or other calibration errors of the position sensors.

potential energy is shaped based only on motor position. Special effort is therefore needed in order to exactly satisfy the control specifications expressed in terms of the link position (such as desired tip position or Cartesian elasticity). This is reflected in the more involved computations needed for implementation of the Cartesian controller from Section 4. The main idea is to define an auxiliary position variable which is a function of $\boldsymbol{\theta}$ only (in order to preserve passivity), but is statically equivalent to the link side position $\boldsymbol{q}$. After understanding this idea, the reader may skip at first reading the rest of the section containing the technical details and the passivity analysis and continue with the experimental part.

3. Joint Level Torque and Position Control

In the following we summarize the approaches adopted for DLR robots for joint level torque and position control and give the unifying, passivity-based view of the problem, which allows further generalization to Cartesian impedance control.

3.1. Passivity-based Joint Position Control

The starting point in the control development was a joint state feedback controller for regulation tasks given by

$$\begin{aligned}\boldsymbol{\tau}_m &= -\boldsymbol{K}_P\tilde{\boldsymbol{\theta}} - \boldsymbol{K}_D\dot{\boldsymbol{\theta}} \\ &\quad +\boldsymbol{K}_T(\boldsymbol{g}(\boldsymbol{q}_d) - \boldsymbol{\tau}) - \boldsymbol{K}_S\dot{\boldsymbol{\tau}} + \boldsymbol{g}(\boldsymbol{q}_d)\end{aligned} \tag{4}$$

with $\boldsymbol{K}_P$, $\boldsymbol{K}_D$, $\boldsymbol{K}_T$, and $\boldsymbol{K}_S$ being positive definite diagonal matrices and with a gravity compensation $\boldsymbol{g}(\boldsymbol{q}_d)$ based on the desired position $\boldsymbol{q}_d$. The error $\tilde{\boldsymbol{\theta}} = \boldsymbol{\theta} - \boldsymbol{\theta}_d$ is computed using a desired value

$$\boldsymbol{\theta}_d = \boldsymbol{q}_d + \boldsymbol{K}^{-1}\boldsymbol{g}(\boldsymbol{q}_d), \tag{5}$$

This constitutes an extension of the PD controller from Tomei (1991) to a full state feedback. Within this section, free motion of the robot is assumed, i.e., $\boldsymbol{\tau}_{\text{ext}} = \boldsymbol{0}$. Under some conditions related to the minimal eigenvalues of $\boldsymbol{K}_P$ and $\boldsymbol{K}_D$ (see Section 3.3 and Appendix B), the controller together with the motor side dynamics (2) can be shown to provide a passive subsystem, which in turn leads to passivity of the entire closed loop system[3] (Albu-Schäffer et al. 2001; Albu-Schäffer 2002), as sketched in Figure 2. In Albu-Schäffer (2002) it was exemplified that by adequately designing the controller gains $\boldsymbol{K}_P$, $\boldsymbol{K}_D$, $\boldsymbol{K}_T$, and $\boldsymbol{K}_S$, the structure can be used to implement a torque, position or impedance controller on joint level (see also Section 3.3). The controller is reformulated and analyzed in the next section in order to allow generalization to the Cartesian case.

3. Passivity is given in this case with respect to the input–output pair $\{\boldsymbol{\tau}_a, \dot{\boldsymbol{q}}\}$.

3.2. Joint Torque Control: Shaping the Actuator Kinetic Energy

In order simplify the analysis and to be able to generalize the joint level approach also to Cartesian coordinates, the idea of interpreting the joint torque feedback as the shaping of the motor inertia plays a central role (Ott et al. 2004). It enables one to use directly the torque feedback within the passivity framework and conceptually divides the controller design into two steps, one related to torque feedback and the other to position feedback. However, in contrast to singular perturbation approaches, the analysis does not require the two loops to have different time scales, which would require very high bandwidth for the torque controller in order to achieve good overall performance.

Consider a torque feedback of the form

$$\boldsymbol{\tau}_m = \boldsymbol{B}\boldsymbol{B}_\theta^{-1}\boldsymbol{u} + (\boldsymbol{I} - \boldsymbol{B}\boldsymbol{B}_\theta^{-1})(\boldsymbol{\tau} + \boldsymbol{D}\boldsymbol{K}^{-1}\dot{\boldsymbol{\tau}}). \tag{6}$$

Herein $\boldsymbol{u} \in \mathbb{R}^n$ is an intermediate control input and $\boldsymbol{B}_\theta$ is a diagonal, positive definite matrix, such that $b_{\theta i} < b_i$. The torque controller leads together with (2) to

$$\boldsymbol{B}_\theta\ddot{\boldsymbol{\theta}} + \boldsymbol{\tau} + \boldsymbol{D}\boldsymbol{K}^{-1}\dot{\boldsymbol{\tau}} = \boldsymbol{u} \tag{7}$$

Comparing (2) with (7) it is clear that the effect of the torque controller is that of reducing the motor inertia to $\boldsymbol{B}_\theta$ for the new subsystem with input $\boldsymbol{u}$.[4]

In order to be able to effectively damp the torque dynamics, (6) can be replaced by a more general version of the torque controller:

$$\begin{aligned}\boldsymbol{\tau}_m &= \boldsymbol{B}\boldsymbol{B}_\theta^{-1}\boldsymbol{u} + \boldsymbol{\tau} + \boldsymbol{D}\boldsymbol{K}^{-1}\dot{\boldsymbol{\tau}} \\ &\quad -\boldsymbol{B}\boldsymbol{B}_\theta^{-1}(\boldsymbol{\tau} + \boldsymbol{D}_s\boldsymbol{K}^{-1}\dot{\boldsymbol{\tau}})\end{aligned} \tag{8}$$

where $\boldsymbol{D}_s$ is an independent diagonal gain matrix for the torque derivative feedback. This is basically a PD torque controller, written in a form which reflects the given physical interpretation. In this case, the new motor dynamics is given by

$$\boldsymbol{B}_\theta\ddot{\boldsymbol{\theta}} + \boldsymbol{\tau} + \boldsymbol{D}_s\boldsymbol{K}^{-1}\dot{\boldsymbol{\tau}} = \boldsymbol{u} \tag{9}$$

Usual values for the ratio $\boldsymbol{B}\boldsymbol{B}_\theta^{-1}$ for the DLR lightweight robots are between 4 and 6 for a compliant behaviour, while lower values are chosen, e.g., for position control, when high stiffness is desired. This ratio (and thus the achievable bandwidth of the torque controller) is determined mainly by the noise level of the torque sensors[5]. Notice that the motor friction is also reduced by the torque feedback, the term $\boldsymbol{\tau}_f$ from (2) would appear in this equation scaled down by $\boldsymbol{B}_\theta\boldsymbol{B}^{-1}$.

4. The controller also scales down by the factor $\boldsymbol{B}_\theta\boldsymbol{B}^{-1}$ any perturbation torque acting on motor side (e.g., the friction torque).

5. Notice, however, that for the flexible joint case, the torque represents a state of the system and is therefore quite smooth, such that a simple first-order low pass filter with cut-off frequency 250 Hz can be used for the DLR robots.

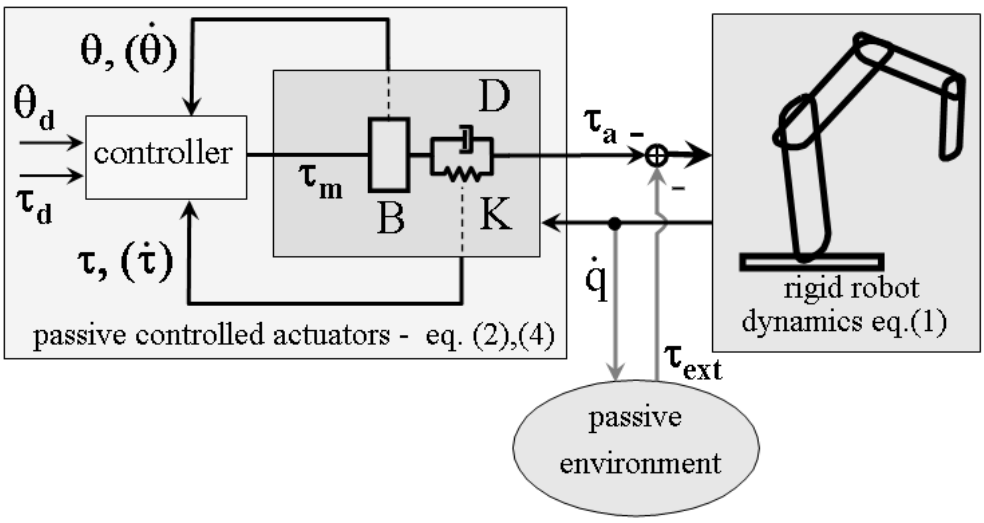

Fig. 2. Representation of the position controlled robot as a connection of passive blocks. The spring torque $\boldsymbol{\tau}$ is measured by a torque sensor and the motor position $\boldsymbol{\theta}$ by an encoder. The derivatives are obtained by numerical differentiation.

3.3. Motor Position-based Feedback: Shaping the Potential Energy

First notice that for the control at joint level, a controller of the form

$$\boldsymbol{u} = -\boldsymbol{K}_\theta\tilde{\boldsymbol{\theta}} - \boldsymbol{D}_\theta\dot{\boldsymbol{\theta}} + \boldsymbol{g}(\boldsymbol{q}_d) \tag{10}$$

with $\tilde{\boldsymbol{\theta}} = \boldsymbol{\theta} - \boldsymbol{\theta}_d$ and $\boldsymbol{K}_\theta$, $\boldsymbol{D}_\theta$ being positive definite gain matrices, is passive with respect to the input–output pair $\{\boldsymbol{u}, \dot{\boldsymbol{\theta}}\}$. Taking into consideration the passivity of all other subsystems, this enables the conclusion of passivity for the entire closed loop system. Actually, the controller (6), (10) can be shown to be equivalent to the formulation (4), with $\boldsymbol{K}_P = \boldsymbol{B}\boldsymbol{B}_\theta^{-1}\boldsymbol{K}_\theta$, $\boldsymbol{K}_D = \boldsymbol{B}\boldsymbol{B}_\theta^{-1}\boldsymbol{D}_\theta$, $\boldsymbol{K}_T = \boldsymbol{B}\boldsymbol{B}_\theta^{-1} - \boldsymbol{I}$, and $\boldsymbol{K}_S = (\boldsymbol{B}\boldsymbol{B}_\theta^{-1} - \boldsymbol{I})\boldsymbol{D}\boldsymbol{K}^{-1}$. For the torque controller (8) one has in turn $\boldsymbol{K}_S = (\boldsymbol{B}\boldsymbol{B}_\theta^{-1}\boldsymbol{D}_s - \boldsymbol{D})\boldsymbol{K}^{-1}$. Based on these passivity properties, asymptotic stability can be shown for the regulation case if some minimal bounds on $\boldsymbol{K}_\theta$ (and also $\boldsymbol{D}_\theta$ for controller (6)) are satisfied, as described in Appendix A.

The controller provides a shaping of the potential energy based only on the motor position $\boldsymbol{\theta}$, such that $\boldsymbol{q}_d$ becomes the only equilibrium point of the potential function. This idea will be extended to the Cartesian impedance control case in Section 4.

3.4. Design of Variable Control Gains

As shown in Appendix A, the Lyapunov function for the position controller is given by

$$\begin{aligned} V(\boldsymbol{w}, \dot{\boldsymbol{w}}) \;=\; & \frac{1}{2}(\dot{\boldsymbol{q}}^T\boldsymbol{M}(\boldsymbol{q})\dot{\boldsymbol{q}} + \dot{\boldsymbol{\theta}}^T\boldsymbol{B}_\theta\dot{\boldsymbol{\theta}}) \\ & + U_P(\boldsymbol{w}) - U_P(\boldsymbol{w}_d) - \frac{\partial U_P(\boldsymbol{w}_d)}{\partial \boldsymbol{w}}(\boldsymbol{w} - \boldsymbol{w}_d), \end{aligned} \tag{11}$$

with $\boldsymbol{w} = (\boldsymbol{\theta}, \boldsymbol{q})$ and with $U_P(\boldsymbol{w}) = U(\boldsymbol{w}) + U_s(\boldsymbol{\theta})$ being the sum of the potential energies of the robot and of the controller. The derivative of $V(\boldsymbol{w}, \dot{\boldsymbol{w}})$ along the system trajectories in the case of the controller (8) is given (see Appendix A)

$$\begin{aligned} \dot{V}_1(\dot{\boldsymbol{w}}) \;=\; & -\dot{\boldsymbol{\theta}}^T\boldsymbol{D}_\theta\dot{\boldsymbol{\theta}} - (\dot{\boldsymbol{\theta}} - \dot{\boldsymbol{q}})^T\boldsymbol{D}(\dot{\boldsymbol{\theta}} - \dot{\boldsymbol{q}}) + \\ & \dot{\boldsymbol{\theta}}^T(\boldsymbol{D} - \boldsymbol{D}_s)(\dot{\boldsymbol{\theta}} - \dot{\boldsymbol{q}}). \end{aligned} \tag{12}$$

Since the linearization of the system around a desired equilibrium point $\boldsymbol{w}_d$ is controllable, a linear full state feedback controller (with gains that can be chosen to arbitrarily assign eigenvalues for the linearized plant around the desired configuration, at least in principle) is indeed often used in practice in order to increase the local performance of standard (PD) controllers for robots with joint flexibility (Lückel et al. 1993; Stelter 2001). For constant control gains, the analysis done above legitimates this choice also from the point of view of global asymptotic stabilization. However, in order to further increase performance, the gains of the controller are sometimes chosen based on gain scheduling, using the actual motor configuration $\boldsymbol{\theta}$ as a scheduling variable. The design of the gains then tries to satisfy the following criteria:

- Minimizing the response time for a given robot configuration
- Provide the desired (well damped) transient behavior
- Limit the control gains to certain (experimentally determined) bounds $\boldsymbol{K}_{i\min} < \boldsymbol{K}_i < \boldsymbol{K}_{i\max}$, which are influenced by the signal-noise level, unmodeled dynamics, actuator saturation, friction uncertainty, etc.

The stability analysis can easily be extended in order to provide a theoretically sound framework also for the case of variable gains. For this, first notice that the matrices $\boldsymbol{D}_\theta$ and $\boldsymbol{D}_s$ enter only $\dot{V}(\boldsymbol{w}, \dot{\boldsymbol{w}})$ and not $V(\boldsymbol{w}, \dot{\boldsymbol{w}})$. Consequently the analysis is valid without modifications if these gains are dependent on the motor side position, i.e., $\boldsymbol{D}_\theta(\boldsymbol{\theta})$, and $\boldsymbol{D}_s(\boldsymbol{\theta})$. Moreover, notice that $\boldsymbol{B}_\theta$ can be chosen state dependent, as $\boldsymbol{B}_\theta(\boldsymbol{\theta})$, if the controller contains an additional term $\dot{\boldsymbol{B}}_\theta(\boldsymbol{\theta})\dot{\boldsymbol{\theta}}$. This term can be seen in analogy to the centripetal and Coriolis vector in (1). It is needed in order to cancel in $\dot{V}(\boldsymbol{w}, \dot{\boldsymbol{w}})$ the term related to the variation of the virtual motor side inertia $\boldsymbol{B}_\theta(\boldsymbol{\theta})$. Finally, also a configuration dependent gain $\boldsymbol{K}_\theta$ can be chosen if $\boldsymbol{K}_\theta(\boldsymbol{\theta})\boldsymbol{\theta}$ is integrable[6]. This, however, is difficult to be satisfied for gains resulting from a general linear design. In conclusion, a possible design procedure is to define a controller of the form

$$\begin{aligned} \boldsymbol{\tau}_m &= \boldsymbol{B}\boldsymbol{B}_\theta^{-1}(\boldsymbol{\theta})\boldsymbol{u} + \boldsymbol{\tau} + \boldsymbol{D}\boldsymbol{K}^{-1}\dot{\boldsymbol{\tau}} \\ &\quad -\boldsymbol{B}\boldsymbol{B}_\theta^{-1}(\boldsymbol{\theta})\left[(\boldsymbol{\tau} + \boldsymbol{D}_s(\boldsymbol{\theta})\boldsymbol{K}^{-1}\dot{\boldsymbol{\tau}}) + \dot{\boldsymbol{B}}_\theta(\boldsymbol{\theta})\dot{\boldsymbol{\theta}}\right] \qquad (13) \\ \boldsymbol{u} &= -\boldsymbol{K}_\theta\tilde{\boldsymbol{\theta}} - \boldsymbol{D}_\theta(\boldsymbol{\theta})\dot{\boldsymbol{\theta}} + \boldsymbol{g}(\boldsymbol{q}_d) \qquad (14) \end{aligned}$$

where only $\boldsymbol{K}_\theta$ is constant and all the other gains are state dependent, resulting from a classical linear design. Then the Lyapunov function as well as its derivative remain unchanged, except for the replacement of $\boldsymbol{K}_\theta$, $\boldsymbol{B}_\theta$, $\boldsymbol{D}_s$ by $\boldsymbol{K}_\theta(\boldsymbol{\theta})$, $\boldsymbol{B}_\theta(\boldsymbol{\theta})$, $\boldsymbol{D}_s(\boldsymbol{\theta})$.

Alternatively, $\boldsymbol{K}_\theta\tilde{\boldsymbol{\theta}}$ can be replaced in (14) by the derivative of any potential function $U_{s\theta}(\boldsymbol{\theta})$ which leads to an unique equilibrium at $\boldsymbol{\theta}_d$:

$$\boldsymbol{u} = -\frac{\partial U_{s\theta}(\boldsymbol{\theta})}{\partial \boldsymbol{\theta}} - \boldsymbol{D}_\theta(\boldsymbol{\theta})\dot{\boldsymbol{\theta}} + \boldsymbol{g}(\boldsymbol{q}_d) \qquad (15)$$

3.5. Tracking Performance

In De Luca (2000) it was mentioned that a simple motor side PD controller can be used together with appropriate feedforward terms also for trajectory tracking. The position controller developed above can be applied in exactly the same way, having the advantage of additionally providing an improved disturbance rejection performance due to the torque feedback.

Using (1) with $\boldsymbol{\tau}_{\text{ext}} = \boldsymbol{0}$, and (3), the desired motor position $\boldsymbol{\theta}_d$ can be obtained from the relations

$$\boldsymbol{K}\boldsymbol{\theta}_d + \boldsymbol{D}\dot{\boldsymbol{\theta}}_d = \boldsymbol{K}\boldsymbol{q}_d + \boldsymbol{D}\dot{\boldsymbol{q}}_d + \boldsymbol{\tau}_{ad}, \qquad (16)$$

$$\boldsymbol{\tau}_{ad} = \boldsymbol{M}(\boldsymbol{q}_d)\ddot{\boldsymbol{q}}_d + \boldsymbol{C}(\boldsymbol{q}_d, \dot{\boldsymbol{q}}_d)\dot{\boldsymbol{q}}_d + \boldsymbol{g}(\boldsymbol{q}_d) \qquad (17)$$

Since $\boldsymbol{D}$ and $\boldsymbol{K}$ are diagonal matrices, $\boldsymbol{\theta}_d$ can be computed for each joint separately and can be implemented online as linear filtering after computing $\boldsymbol{\tau}_{ad}$. From (6), (7) evaluated along the desired motion, the feed-forward command $\boldsymbol{u}_{\text{ff}}$ can be computed as

$$\boldsymbol{u}_{\text{ff}} = \boldsymbol{B}_\theta\ddot{\boldsymbol{\theta}}_d + \boldsymbol{\tau}_{ad}. \qquad (18)$$

The feedforward command includes through $\ddot{\boldsymbol{\theta}}_d$ the derivatives of $\boldsymbol{q}_d$ up to fourth order, which therefore have to be provided as smooth functions of time. In this case, (14) is replaced by

$$\boldsymbol{u} = -\boldsymbol{K}_\theta\tilde{\boldsymbol{\theta}} - \boldsymbol{D}_\theta(\boldsymbol{\theta})\dot{\tilde{\boldsymbol{\theta}}} + \boldsymbol{u}_{\text{ff}}, \qquad (19)$$

with $\dot{\tilde{\boldsymbol{\theta}}} = \dot{\boldsymbol{\theta}} - \dot{\boldsymbol{\theta}}_d$. Only local stability results along the trajectory can be shown for such a controller. This is, however, practically sufficient for trajectory tracking with high gains $\boldsymbol{K}_\theta$ and initial tracking error close to zero. For global tracking convergence, a controller has to include also the higher derivatives of $\boldsymbol{q}$, as mentioned in Section 1.

4. Impedance Control

While the structure presented so far can be effectively used for position control, it has two major drawbacks when used for impedance control. First, as mentioned in Appendix A, some minimal values for $\boldsymbol{K}_\theta$ (or $\boldsymbol{K}_P$) have to be ensured in order to prove the asymptotic stability. This is related to the fact that the gravity compensation is done based on the desired position. For impedance control, however, the desired stiffness may be arbitrarily close to zero, making gravity compensation based on desired position not meaningful. Second, the desired stiffness relation can be satisfied only locally by controllers of the type given by (10), due to additional variation of the gravity term and, in the Cartesian version, of the Jacobian. In order to see this more clearly, consider the equilibrium equations[7]

$$\begin{aligned} \boldsymbol{K}(\boldsymbol{\theta} - \boldsymbol{q}) &= \boldsymbol{g}(\boldsymbol{q}) - \boldsymbol{\tau}_{\text{ext}} \\ \boldsymbol{K}(\boldsymbol{\theta} - \boldsymbol{q}) + \boldsymbol{K}_\theta\tilde{\boldsymbol{\theta}} &= \boldsymbol{0} \end{aligned}$$

of the robot with the controller (10). By eliminating $\boldsymbol{\theta}$, one obtains

$$\boldsymbol{\tau}_{\text{ext}} = \boldsymbol{g}(\boldsymbol{q}) + \boldsymbol{K}(\boldsymbol{K} + \boldsymbol{K}_\theta)^{-1}\boldsymbol{K}_\theta(\boldsymbol{q} - \boldsymbol{\theta}_d)$$

The output stiffness $\boldsymbol{K}_q$ which results for this controller is thus

$$\boldsymbol{K}_q = \frac{\partial \boldsymbol{\tau}_{\text{ext}}}{\partial \boldsymbol{q}} = \frac{\partial \boldsymbol{g}(\boldsymbol{q})}{\partial \boldsymbol{q}} + \boldsymbol{K}(\boldsymbol{K} + \boldsymbol{K}_\theta)^{-1}\boldsymbol{K}_\theta, \qquad (20)$$

and is hence position dependent. In the next subsection an approach is presented, which overcomes the mentioned shortcomings. The main idea is to design the outer loop by introducing a new control variable $\bar{\boldsymbol{q}}$, which is a function of the

6. Then U_s is given by this integral, which defines a potential for the vector field $\boldsymbol{K}_\theta(\boldsymbol{\theta})\boldsymbol{\theta}$ such that $\frac{\partial U_s(\boldsymbol{\theta})}{\partial \boldsymbol{\theta}} = \boldsymbol{K}_\theta(\boldsymbol{\theta})\boldsymbol{\theta}$.

7. Obtained for a constant $\boldsymbol{\tau}_{\text{ext}}$ from (1), (2), (3), (7), (10) by setting all derivatives to zero.

collocated (motor) position $\boldsymbol{\theta}$ only, but is equal to the noncollocated position $\boldsymbol{q}$ (link side) in every static configuration. An iterative computation method based on the contraction mapping theorem is used to calculate this variable. The outer loop controller designed in this way can be shown to be passive, while exactly fulfilling all the steady state requirements for the system. These include not only the desired equilibrium position, but also the exact stiffness relationship between the end-effector position and the external force. The approach can be interpreted as a shaping of the potential energy of the robot.

4.1. The Cartesian Case: Implementing Exact Desired Stiffness

In this section, the more general case of Cartesian impedance control is treated. In contrary to position or force control in which the control goal is to follow a given setpoint (for position or force respectively), the goal of impedance control is to achieve a closed loop behavior which resembles a given impedance behavior (Hogan 1985). The analysis treats a desired impedance which is characterized by a desired stiffness and damping behavior, while link side inertia shaping is not treated. This type of impedance control is sometimes also referred to as compliance control. The joint level impedance controller can be easily derived from it. In analogy to rigid robot impedance control (Hogan 1985), a first choice for the outer loop controller would be:

$$\boldsymbol{u} = -\boldsymbol{J}(\boldsymbol{q})^T(\boldsymbol{K}_x\tilde{\boldsymbol{x}}(\boldsymbol{q}) + \boldsymbol{D}_x\dot{\boldsymbol{x}}(\boldsymbol{q})) + \boldsymbol{g}(\boldsymbol{q}), \quad (21)$$

$$\tilde{\boldsymbol{x}}(\boldsymbol{q}) = \boldsymbol{f}(\boldsymbol{q}) - \boldsymbol{x}_d. \quad (22)$$

Herein, $\boldsymbol{x}_d$ is the constant desired end-effector pose and $\boldsymbol{x}(\boldsymbol{q}) = \boldsymbol{f}(\boldsymbol{q})$ is the end-effector pose computed by the direct kinematics map $\boldsymbol{f}$. $\boldsymbol{J}(\boldsymbol{q}) = \frac{\partial \boldsymbol{f}(\boldsymbol{q})}{\partial \boldsymbol{q}}$ is the manipulator Jacobian. $\boldsymbol{K}_x$ and $\boldsymbol{D}_x$ are positive definite matrices for the desired stiffness and damping. The equilibrium conditions are then given by[8]

$$\boldsymbol{K}(\boldsymbol{\theta}_0 - \boldsymbol{q}_0) = \boldsymbol{g}(\boldsymbol{q}_0) - \boldsymbol{J}(\boldsymbol{q}_0)^T\boldsymbol{F}_{\text{ext}} \quad (23)$$

$$\boldsymbol{K}(\boldsymbol{\theta}_0 - \boldsymbol{q}_0) + \boldsymbol{J}(\boldsymbol{q}_0)^T\boldsymbol{K}_x\tilde{\boldsymbol{x}}(\boldsymbol{q}_0) = \boldsymbol{g}(\boldsymbol{q}_0), \quad (24)$$

where the relation $\boldsymbol{\tau}_{\text{ext}} = \boldsymbol{J}(\boldsymbol{q}_0)^T\boldsymbol{F}_{\text{ext}}$ between the external joint torque and the external force $\boldsymbol{F}_{\text{ext}}$ acting from the environment on the robot end-effector was used. Obviously, this leads to the desired stiffness relation $\boldsymbol{F}_{\text{ext}} = \boldsymbol{K}_x\tilde{\boldsymbol{x}}$ in any equilibrium position as long as $\boldsymbol{J}(\boldsymbol{q}_0)$ has full column rank.

It is well known that the system (1) is passive with respect to the input–output pair $\{\boldsymbol{\tau}_a + \boldsymbol{\tau}_{\text{ext}}, \dot{\boldsymbol{q}}\}$. This can be shown with the storage function $S_q = \frac{1}{2}\dot{\boldsymbol{q}}^T\boldsymbol{M}(\boldsymbol{q})\dot{\boldsymbol{q}} + V_g(\boldsymbol{q})$, where $V_g(\boldsymbol{q})$ is a potential function for $\boldsymbol{g}(\boldsymbol{q})$. In order to ensure the passivity of the complete system, we are now looking for a control law for $\boldsymbol{u}$ which determines (7) to be passive in $\{\dot{\boldsymbol{q}}, -\boldsymbol{\tau}_a\}$. Obviously, (21) does not satisfy the required passivity condition. The usual solution adopted in Tomei (1991), Albu-Achäffer et al. (2001), Zollo et al. (2005), Ott et al. (2004), Albu-Schäffer et al. (2004b) in order to ensure the passivity in $\{\dot{\boldsymbol{q}}, -\boldsymbol{\tau}_a\}$ is to chose $\boldsymbol{u}$ as a function of $\boldsymbol{\theta}$ and its derivative only. Then the controller is passive with respect to $\{\dot{\boldsymbol{\theta}}, -\boldsymbol{u}\}$ and is further connected to the passive motor side dynamics, thus satisfying the desired property[9]. The basic idea for the solution proposed in this paper uses the fact that, under some mild conditions, there is a one to one mapping $\boldsymbol{\theta}_0 = \boldsymbol{h}(\boldsymbol{q}_0)$ at equilibrium points (in our case through (24)) between $\boldsymbol{\theta}_0$ and $\boldsymbol{q}_0$:

$$\boldsymbol{\theta}_0 = \boldsymbol{h}(\boldsymbol{q}_0) = \boldsymbol{q}_0 + \boldsymbol{K}^{-1}\boldsymbol{l}(\boldsymbol{q}_0), \quad (25)$$

$$\text{with } \boldsymbol{l}(\boldsymbol{q}_0) = -\boldsymbol{J}(\boldsymbol{q}_0)^T\boldsymbol{K}_x\tilde{\boldsymbol{x}}(\boldsymbol{q}_0) + \boldsymbol{g}(\boldsymbol{q}_0). \quad (26)$$

The proposed solution consists in replacing $\boldsymbol{q}$ in (21) with its static equivalent $\bar{\boldsymbol{q}}(\boldsymbol{\theta}) = \boldsymbol{h}^{-1}(\boldsymbol{\theta})$, which is based only on the motor position. One obtainins the following controller, which is *statically equivalent* to (21):

$$\boldsymbol{u} = -\boldsymbol{J}(\bar{\boldsymbol{q}})^T(\boldsymbol{K}_x\tilde{\boldsymbol{x}}(\bar{\boldsymbol{q}}) + \boldsymbol{D}_x\boldsymbol{J}(\bar{\boldsymbol{q}})\dot{\boldsymbol{\theta}}) + \boldsymbol{g}(\bar{\boldsymbol{q}}) \quad (27)$$

$$\tilde{\boldsymbol{x}}(\bar{\boldsymbol{q}}) = \boldsymbol{f}(\bar{\boldsymbol{q}}) - \boldsymbol{x}_d. \quad (28)$$

Since $\bar{\boldsymbol{q}}(\boldsymbol{\theta}_0) = \boldsymbol{q}_0$ holds at rest, it follows that the equilibrium (23),(24) and thus the desired static relation $\boldsymbol{F}_{\text{ext}} = \boldsymbol{K}_x\tilde{\boldsymbol{x}}(\boldsymbol{q}_0)$ is still valid for this new controller. This basic idea was introduced in Ott et al (2004) and Albu-Schäffer et al. (2004) for the case of gravity compensation only and was generalized in Albu-Schäffer (2004a) in order to provide an exact link side Cartesian stiffness. The closed loop dynamics of the system results from (1), (7), and (27):

$$\boldsymbol{M}(\boldsymbol{q})\ddot{\boldsymbol{q}} + \boldsymbol{C}(\boldsymbol{q},\dot{\boldsymbol{q}})\dot{\boldsymbol{q}} + \boldsymbol{g}(\boldsymbol{q}) = \boldsymbol{\tau}_a + \boldsymbol{\tau}_{\text{ext}} \quad (29)$$

$$\boldsymbol{B}_\theta\ddot{\boldsymbol{\theta}} - \boldsymbol{l}(\bar{\boldsymbol{q}}) + \boldsymbol{J}(\bar{\boldsymbol{q}})^T\boldsymbol{D}_x\boldsymbol{J}(\bar{\boldsymbol{q}})\dot{\boldsymbol{\theta}} + \boldsymbol{\tau}_a = \boldsymbol{0} \quad (30)$$

REMARK 1. While in general the inverse function $\boldsymbol{h}^{-1}$ cannot be computed analytically, for a given $\boldsymbol{\theta}$ it is possible to approximate the value $\bar{\boldsymbol{q}} = \boldsymbol{h}^{-1}(\boldsymbol{\theta})$ with arbitrary accuracy by iteration in the case that the mapping $\boldsymbol{T}(\boldsymbol{q}) := \boldsymbol{\theta} - \boldsymbol{K}^{-1}\boldsymbol{l}(\boldsymbol{q})$ is a contraction. The mapping $\boldsymbol{T}(\boldsymbol{q})$ has then a unique fixed-point $\boldsymbol{q}^* = \boldsymbol{T}(\boldsymbol{q}^*) = \bar{\boldsymbol{q}}$. The iteration

$$\hat{\boldsymbol{q}}_{n+1} = \boldsymbol{T}(\hat{\boldsymbol{q}}_n) \quad (31)$$

converges thus for every starting point[10] to this fixed-point, as follows from the contraction mapping theorem (see Vidyasagar 1978):

$$\lim_{n\to\infty}\hat{\boldsymbol{q}}_n = \boldsymbol{q}^* = \bar{\boldsymbol{q}}. \quad (32)$$

8. $\boldsymbol{\theta}_0$ and $\boldsymbol{q}_0$ stand for the equilibrium values of $\boldsymbol{\theta}$ and $\boldsymbol{q}$.

9. In order to have an overview of the causality of the various blocks as well as on the signs of the involved input–output pairs, a first short look at Figure 3, displaying the final controller structure, might be useful.

10. E.g., one can choose $\hat{\boldsymbol{q}}_0 = \boldsymbol{\theta}$ or alternatively $\hat{\boldsymbol{q}}_0$ equal to the result of the iteration during the previous control cycle.

In order for $\boldsymbol{T}(\boldsymbol{q})$ to be a contraction, it is sufficient to show that there exists an $\alpha \in \mathbb{R}$ satisfying:

$$\left|\left|\frac{\partial \boldsymbol{l}(\boldsymbol{q})}{\partial \boldsymbol{q}}\right|\right| \leq \alpha < \frac{1}{||\boldsymbol{K}^{-1}||} \quad \forall \boldsymbol{q} \in \mathbb{R}^n. \tag{33}$$

This implies the following inequality:

$$||\boldsymbol{l}(\boldsymbol{q}_1) - \boldsymbol{l}(\boldsymbol{q}_2)|| \leq \alpha ||\boldsymbol{q}_1 - \boldsymbol{q}_2||, \quad \forall \boldsymbol{q}_1, \boldsymbol{q}_2 \in \mathbb{R}^n \tag{34}$$

As a consequence of (34) it follows that

$$\begin{aligned} ||\boldsymbol{T}_1(\boldsymbol{q}_1) - \boldsymbol{T}_1(\boldsymbol{q}_2)|| &\leq ||\boldsymbol{K}^{-1}|| ||\boldsymbol{l}(\boldsymbol{q}_1) - \boldsymbol{l}(\boldsymbol{q}_2)|| \\ &< ||\boldsymbol{q}_1 - \boldsymbol{q}_2|| \end{aligned}$$

The condition (33) can always be fulfilled for a sufficiently small $||\boldsymbol{K}_x||$. A physical interpretation can be given as follows: ignoring gravity, the condition states that the desired Cartesian stiffness, transformed to joint space (Chen and Kao 2000) may not exceed the joint stiffness. This is intuitive, since the overall stiffness results from the serial interconnection of the joint stiffness and the controller stiffness and is therefore lower than any of the two. On the other hand, in the absence of external forces, the condition states that the joint stiffness should be high enough to sustain the robot in the gravity field if the motor is fixed, which is rather self-evident. In the following it is therefore assumed that $\bar{\boldsymbol{q}}$ is known exactly. In practice, good results are obtained by the first or second iteration step. In particular notice that by a first-order approximation with $\hat{\boldsymbol{q}}_0 = \boldsymbol{q}_d$ one would obtain the second version of the controller from Zollo et al. (2005).

REMARK 2. From the remark above it follows that in order to preserve the passivity (and hence the robustness) of the presented control approach, the physical joint stiffness is an upper bound for the achievable closed loop stiffness. Therefore, this controller is not well suited to systems which are designed to be very compliant, such as the series elastic actuators (Pratt and Williamson 1995) for which an increase of the total stiffness has to be accomplished by control. However, the method is a good choice for lightweight robotic structures with cable-driven actuators or harmonic drive gears.

4.2. Comparison with the Joint Impedance Control Version

For the joint impedance control case, the desired equilibrium equations (23), (24) reduce to

$$\boldsymbol{K}(\boldsymbol{\theta}_0 - \boldsymbol{q}_0) = \boldsymbol{g}(\boldsymbol{q}_0) - \boldsymbol{\tau}_{\text{ext}} \tag{35}$$

$$\boldsymbol{K}(\boldsymbol{\theta}_0 - \boldsymbol{q}_0) + \boldsymbol{K}_{q_d}\tilde{\boldsymbol{q}}_0 = \boldsymbol{g}(\boldsymbol{q}_0), \tag{36}$$

where $\boldsymbol{K}_{q_d}$ is the desired link side joint stiffness[11] and $\tilde{\boldsymbol{q}}_0 = \boldsymbol{q} - \boldsymbol{q}_d$. The second relation provides again an implicit equation in $\boldsymbol{q}$. It can be solved numerically in order to obtain $\bar{\boldsymbol{q}}(\boldsymbol{\theta})$ if a condition of the type (33) is satisfied, with

$$\boldsymbol{l}_1(\boldsymbol{q}_0) = -\boldsymbol{K}_{q_d}\tilde{\boldsymbol{q}}_0 + \boldsymbol{g}(\boldsymbol{q}_0). \tag{37}$$

The resulting controller, namely

$$\boldsymbol{u} = -\boldsymbol{K}_{q_d}(\bar{\boldsymbol{q}}(\boldsymbol{\theta}) - \boldsymbol{q}_d) - \boldsymbol{D}_\theta\dot{\boldsymbol{\theta}} + \boldsymbol{g}(\bar{\boldsymbol{q}}(\boldsymbol{\theta})), \tag{38}$$

is an extension of (10), where online gravity compensation was used instead of a compensation based on the desired position and which now exactly implements the desires stiffness matrix $\boldsymbol{K}_{q_d}$.

4.3. Passivity Analysis of the Cartesian Impedance Controller

The passivity of (30) with respect to $\{\dot{\boldsymbol{q}}, -\boldsymbol{\tau}_a\}$ can be shown using the following storage function:

$$S_\theta = \frac{1}{2}\dot{\boldsymbol{\theta}}^T\boldsymbol{B}_\theta\dot{\boldsymbol{\theta}} + \frac{1}{2}(\boldsymbol{\theta} - \boldsymbol{q})^T\boldsymbol{K}(\boldsymbol{\theta} - \boldsymbol{q}) - V_{\bar{l}}(\boldsymbol{\theta}), \tag{39}$$

where $V_{\bar{l}}(\boldsymbol{\theta})$ is the potential function for $\bar{\boldsymbol{l}}(\boldsymbol{\theta}) = \boldsymbol{l}(\bar{\boldsymbol{q}}(\boldsymbol{\theta}))$. It should be mentioned that the potential function for $\boldsymbol{l}(\bar{\boldsymbol{q}}(\boldsymbol{\theta}))$ with $\boldsymbol{\theta}$ as an argument is required in (39), satisfying $\frac{\partial V_{\bar{l}}(\boldsymbol{\theta})}{\partial \boldsymbol{\theta}} = \bar{\boldsymbol{l}}(\boldsymbol{\theta})^T = \boldsymbol{l}(\bar{\boldsymbol{q}}(\boldsymbol{\theta}))^T$. A potential function $V_l(\bar{\boldsymbol{q}})$ in $\bar{\boldsymbol{q}}$, (with $\frac{\partial V_l(\bar{\boldsymbol{q}})}{\partial \bar{\boldsymbol{q}}} = \boldsymbol{l}(\bar{\boldsymbol{q}})^T$) can easily be found:

$$V_l(\bar{\boldsymbol{q}}) = -\frac{1}{2}\tilde{\boldsymbol{x}}^T(\bar{\boldsymbol{q}})\boldsymbol{K}_x\tilde{\boldsymbol{x}}(\bar{\boldsymbol{q}}) + V_g(\bar{\boldsymbol{q}}). \tag{40}$$

In Albu-Schäffer et al. (2004a) it has been shown that the required potential function $V_{\bar{l}}(\boldsymbol{\theta})$ is related to $V_l(\bar{\boldsymbol{q}})$ through

$$V_{\bar{l}}(\boldsymbol{\theta}) = V_l(\bar{\boldsymbol{q}}(\boldsymbol{\theta})) + \frac{1}{2}\boldsymbol{l}^T(\bar{\boldsymbol{q}}(\boldsymbol{\theta}))\boldsymbol{K}^{-1}\boldsymbol{l}(\bar{\boldsymbol{q}}(\boldsymbol{\theta})). \tag{41}$$

For robots with rotational joints, $V_g(\bar{\boldsymbol{q}})$ is upper bounded. By substituting (41) and (40) into (39), it follows that S_θ is bounded from below since all other terms are positive (quadratic). Thus S_θ represents an appropriate storage function.

The time derivative of (39) along the solutions of (30) is:

$$\begin{aligned} \dot{S}_\theta = &-\dot{\boldsymbol{\theta}}^T\boldsymbol{J}^T(\bar{\boldsymbol{q}})\boldsymbol{D}_x\boldsymbol{J}(\bar{\boldsymbol{q}})\dot{\boldsymbol{\theta}} - (\dot{\boldsymbol{\theta}} - \dot{\boldsymbol{q}})^T\boldsymbol{D}(\dot{\boldsymbol{\theta}} - \dot{\boldsymbol{q}}) \\ &-\dot{\boldsymbol{q}}^T\boldsymbol{\tau}_a. \end{aligned}$$

The last term represents the exchanged power of the subsystem and the other terms are negative definite dissipation terms. This shows that the subsystem is indeed passive with respect to $\{\dot{\boldsymbol{q}}, -\boldsymbol{\tau}_a\}$. If the robot is contacting an environment which is also passive (with respect to $\{\dot{\boldsymbol{q}}, -\boldsymbol{\tau}_{\text{ext}}\}$), then the passivity of the entire system is given as a parallel and feedback interconnection of passive subsystems (Figure 3).

As already mentioned, the results of the passivity analysis have important implications for the robot interaction with

11. The desired Cartesian stiffness $\boldsymbol{K}_x$ is now replaced by $\boldsymbol{K}_{q_d}$.

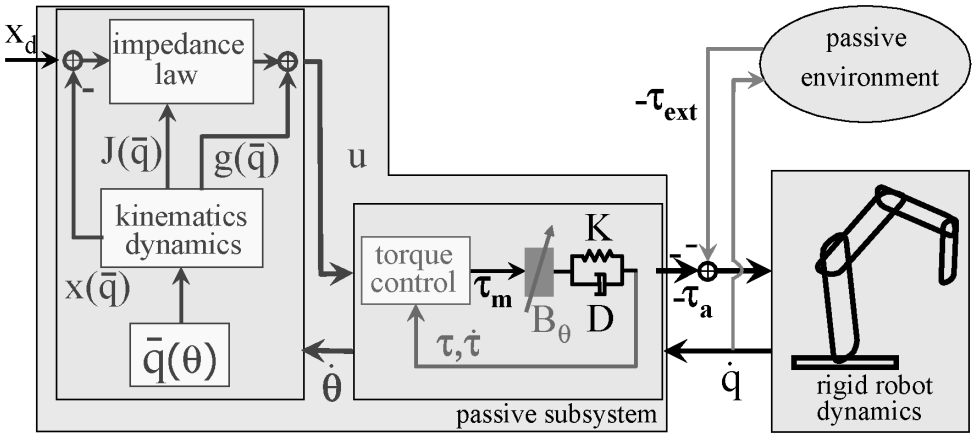

Fig. 3. Representation of the Cartesian impedance controller as parallel and feedback interconnection of passive systems.

the environment. Without going into details it should be mentioned that the storage functions from the passivity analysis can be used also as a Lyapunov function for the proof of asymptotic stability in the case of free motion (Albu-Schäffer et al. 2004a) for a non-redundant manipulator. For redundant manipulators such as the DLR lightweight robots all the passivity properties are valid, while only convergence of the tip position is ensured by the Cartesian controller, the null-space position can be arbitrary at rest. In order to ensure asymptotic convergence in the sense of Lyapunov to a certain joint configuration, an additional null-space stiffness has to be added (Albu-Schäffer et al. 2003).

A last comment on the type of resulting convergence properties should be made. While for the joint impedance control case global convergence results can be obtained, only local statements can be made for the Cartesian case. One reason is the fact that the contraction condition (33) is satisfied globally for $\boldsymbol{l}_1$ if the joint stiffness is higher than the (bounded) Hessian of the gravity potential energy, while it can be satisfied only locally for $\boldsymbol{l}$. A second reason is more fundamental and is related to the robot kinematics properties. Even in the non-redundant, nonsingular case, the Cartesian coordinates describe the configuration of the robot only locally (Burdick 1995). A cuspidal robot (Wenger 1998) can generally converge to the same Cartesian pose but it may reach it with (e.g., two) different joint configurations even without passing a singularity during such a reconfiguration.

4.4. Cartesian Force Command, Redundancy and Singularity Treatment

The way in which a Cartesian force can be implemented within this framework (e.g., for Cartesian hybrid force-position control) should be mentioned here for sake of completeness. A desired Cartesian force $\boldsymbol{F}_d$ can be achieved not only by using impedance control and commanding an appropriate desired point beyond the contact surface (Hogan 1985), but also by setting the desired Cartesian stiffness to zero in the given direction, commanding a desired torque $\boldsymbol{\tau}_d = \boldsymbol{J}^T(\bar{\boldsymbol{q}})\boldsymbol{F}_d$ and adding it to $\boldsymbol{u}$ in (27). Then the local torque controller is used to compensate for disturbances such as friction instead of a Cartesian force controller.

Based on the torque interface, well known methods used to deal with singularities and redundancy can be adapted from the rigid case, e.g., from Khatib (1995). A redundancy treatment within the singular perturbation framework was described in Albu-Schäffer et al. (2003).

5. Experimental Evaluation

First, some experimental results regarding the position control are given for a rest to rest movement of joint 2 of the LWR III, with a rectangular velocity profile. Figure 4 shows a comparison between the controller defined by (19), (8) and two PD controllers, which are obtained by setting $\boldsymbol{B}_\theta = \boldsymbol{B}$, i.e., setting the feedback gains $\boldsymbol{K}_T$ and $\boldsymbol{K}_S$ for the torque and the torque derivative to zero and using only the position and velocity feedback. The higher order derivatives of the desired trajectory in (18) have to be omitted due to the discontinuity of the desired velocity signal. In order to have a direct correspondence to the PD controllers, all gains will be also listed in the equivalent notations of (4), i.e., using $(\boldsymbol{K}_P, \boldsymbol{K}_D, \boldsymbol{K}_T, \boldsymbol{K}_S)$ instead of $(\boldsymbol{B}_\theta, \boldsymbol{D}_s, \boldsymbol{K}_\theta, \boldsymbol{D}_\theta)$, see also Section 3.3 for the correspondence. The parameters of the joint are $b_2 = 3.933$ kgm^2, $k_2 = 21900$ N/m, $d_2 = 9.62$ Nm s/rad and in the considered arm configuration the diagonal term of the mass matrix is $m_{22} = 7.45$ kgm^2. The control gains used

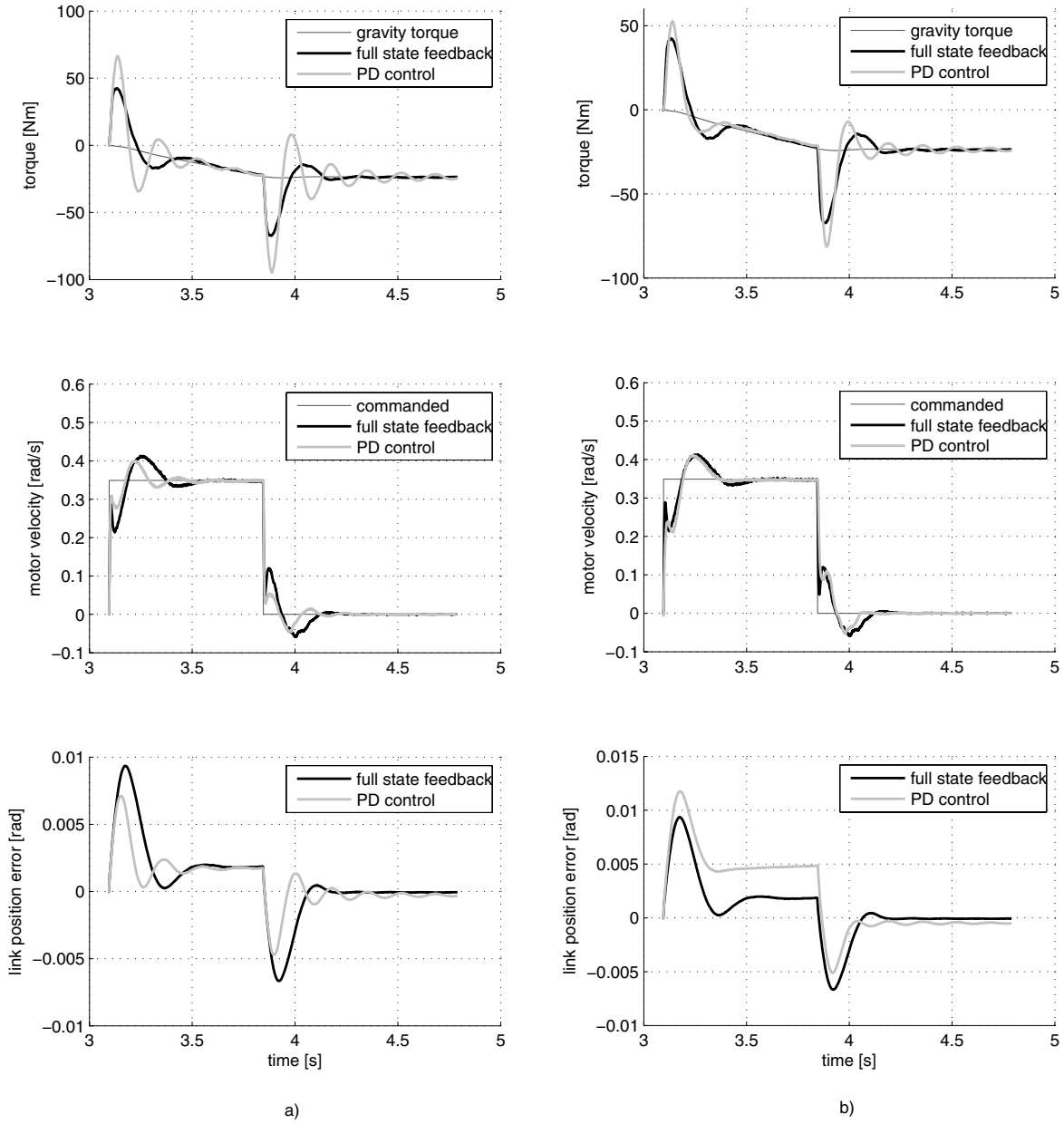

Fig. 4. PD versus state feedback control. Left (a): the gains of the PD controller are identical to the position and velocity feedback gains of the state feedback controller. The PD controlled robot exhibits oscillations. Right (b): The gains of the PD controller are reduced, such that both controllers have the same link side stiffness. The PD controller has higher position errors and still some oscillations on the torque signal.

Table 1. Gains for the Position Controllers

	K_T	K_S	K_P	K_D	K_θ	D_θ
State feedback	2.0	0.01	12000	811.0	4000	270.3
PD from Fig. 4(a)	0.0	0.0	12000	811.0	12000	811.0
PD from Fig. 4(b)	0.0	0.0	4000	270.3	4000	270.3

in the experiments are listed in Table 1. The gains $\boldsymbol{K}_P$ and $\boldsymbol{K}_D$ of the PD controller in Figure 4(a) are the same as for the state feedback controller. The position error is in this case similar, but the PD controlled moves with unacceptable oscillations, as it can be observed on the torque signal. In Figure 4(b), the position feedback for the PD controller is decreased in order to achieve the same link side stiffness, given by (20), as for the state feedback controller. It can be easily verified, that in this case both controllers have the same values for $\boldsymbol{K}_\theta$ and $\boldsymbol{D}_\theta$. The response times of the state feedback controller and of the PD controller from Figure 4(b) are similar, but for the PD controller the position error is considerably larger and the oscillations are still present on the torque signal at the end of the trajectory.

Figure 5 compares a state feedback controller with fixed gains with a variable gain controller on the first axis. During this experiment, the second axis was moved from 90.0 deg to 0.0 deg, causing a continuous decrease of the link inertia for the first axis from 10.277 kgm^2 to 0.1 kgm^2. Although the fixed gain controller proves to work surprisingly well, one can achieve higher bandwidth for low inertia by varying the gains, as described in Section 3.4. In this way, the maximal available motor torque is better exploited.

A typical impact experiment with the 7-dof DLR-lightweight robot II is described next, in order to illustrate the performance of the Cartesian impedance controller. For the experiment a diagonal form of the Cartesian stiffness matrix $\boldsymbol{K}_x$, with the values of Table 2, was chosen. In the experiment a desired trajectory $z_d(t)$ along the vertical z-axis of the end-effector frame was commanded such that the robot hit a wooden surface. During this impact, the Cartesian contact force was measured by a 6-dof force-torque sensor[12]. The measurement of the external forces was done here only for the evaluation, but is not needed for implementation of the controller. Furthermore, the end-effector coordinate $z(\boldsymbol{q})$ was computed from the link side angles $\boldsymbol{q} = \boldsymbol{\theta} + \boldsymbol{K}^{-1}\boldsymbol{\tau}$. The resulting motion $z(\boldsymbol{q})$ and the contact force F_z of the end-effector in z-direction are shown in Figure 6. In order to evaluate the resulting impedance relationship, the ratio $\frac{F_z}{z_d - z(\boldsymbol{q})}$ was computed as an estimation of the stiffness[13]. This estimation is of course only valid in the steady state. The result is shown in Figure 7. At the steady state the estimated stiffness nearly reaches the desired value of 4000 N/m. The remaining difference lies in the range of known stiction effects for this robot.

12. A JR3-sensor was used, with a first- order analog filter at 500 Hz and no additional digital filtering.

13. Beginning at time 0.5s, when the robot movement started.

6. Applications

In this section, some applications based on the presented controllers are shortly presented.

Piston Insertion

Teaching by demonstration is a typical application for impedance controllers. A practical demonstration was given with the task of teaching and automatic insertion of a piston into a motor block. Teaching is realized by guiding the robot with the human hand (Figure 8). It was initially known that the axes of the holes in the motor block were vertically oriented. In the teaching phase, high stiffness components for the orientations were commanded (150 Nm/rad), while the translational stiffness was set to zero. This allowed only translational movements to be demonstrated by the human operator. In the second phase, the taught trajectory has been automatically reproduced by the robot. In this phase, high values were assigned for the translational stiffness (3000 N/m), while the stiffness for the rotations was low (60 Nm/rad). This enabled the robot to compensate for the remaining position errors. For two pistons, the total time for the assembly was 6 s. In this experiment, the assembly was executed automatically four times faster than by the human operator holding the robot as an input device in the teaching phase (24 s), while the free-hand execution of the task by a human requires about 4 s (Extension 1). The insertion task has previously been implemented by using an industrial robot and a compliant force-torque sensor. Despite a well tuned Cartesian force controller, the insertion process had to be performed much slower, because of the well known control problems which occur in the case of hard contacts with conventional robots. Thus, the advantage of a compliant manipulator with stiffness control in assembly tasks is obvious.

Wiping the Table

Here the demand for compliant behaviour of the robot arises from reasons of safety for humans interacting with it, while the contact with the environment (table) was quite soft due to the cloth and hence not as challenging as in the case of

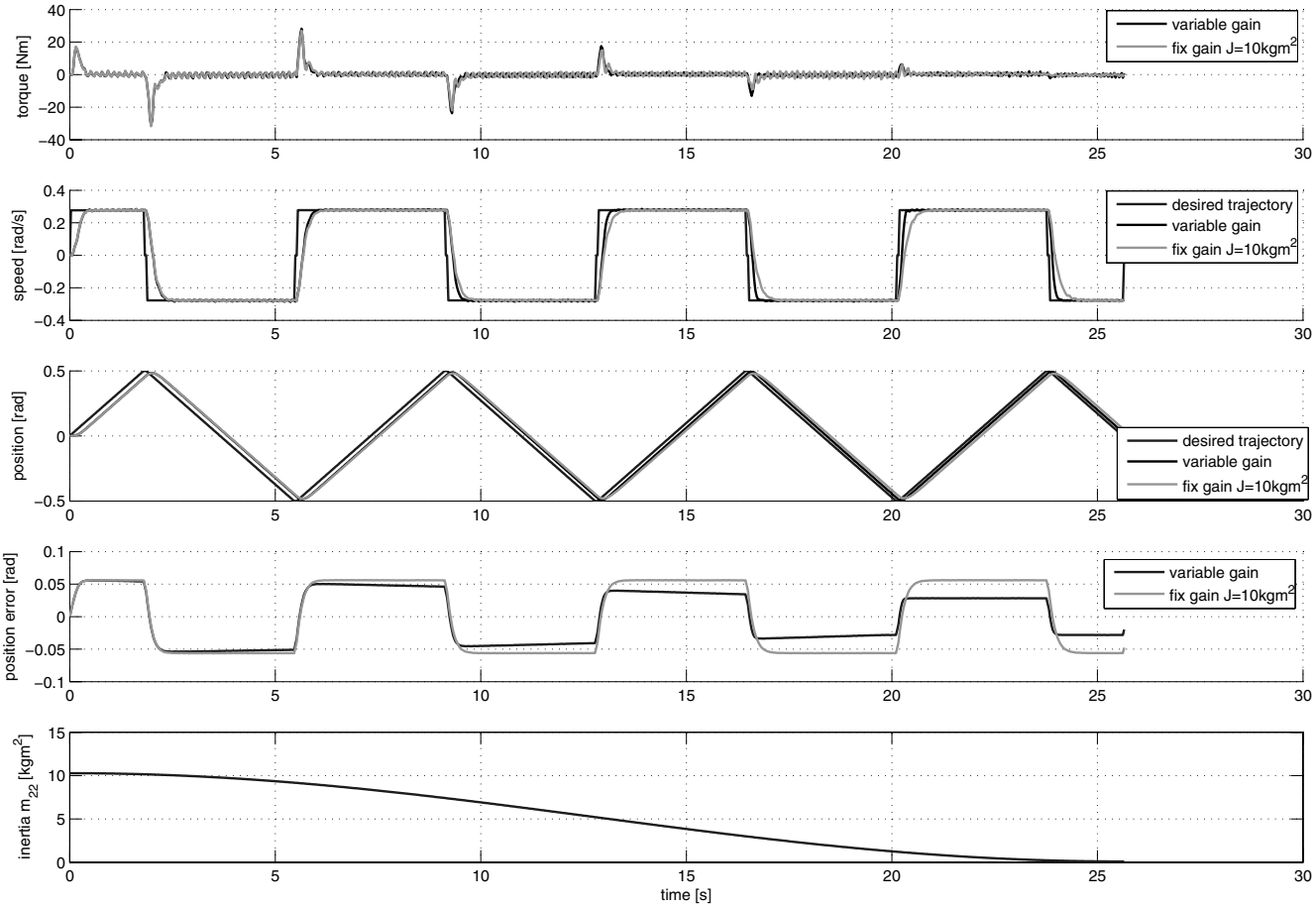

Fig. 5. Fixed gain and variable gain controller for joint 1 of LWRII. The link inertia corresponding to the first joint is continuously decreased from $10.277\,\mathrm{kgm}^2$ to $0.1\,\mathrm{kgm}^2$ due to the simultaneous movement of joint 2. The variable gain controller has faster response time for low inertia.

Table 2. Chosen Values for the Diagonal Cartesian Stiffness Matrix

x	y	z	roll	pitch	yaw
4000	4000	4000	300	300	300
$\frac{\mathrm{Nm}}{\mathrm{rad}}$	$\frac{\mathrm{Nm}}{\mathrm{rad}}$	$\frac{\mathrm{Nm}}{\mathrm{rad}}$			
$\frac{\mathrm{N}}{\mathrm{m}}$	$\frac{\mathrm{N}}{\mathrm{m}}$	$\frac{\mathrm{N}}{\mathrm{m}}$	$\frac{\mathrm{Nm}}{\mathrm{rad}}$	$\frac{\mathrm{Nm}}{\mathrm{rad}}$	$\frac{\mathrm{Nm}}{\mathrm{rad}}$

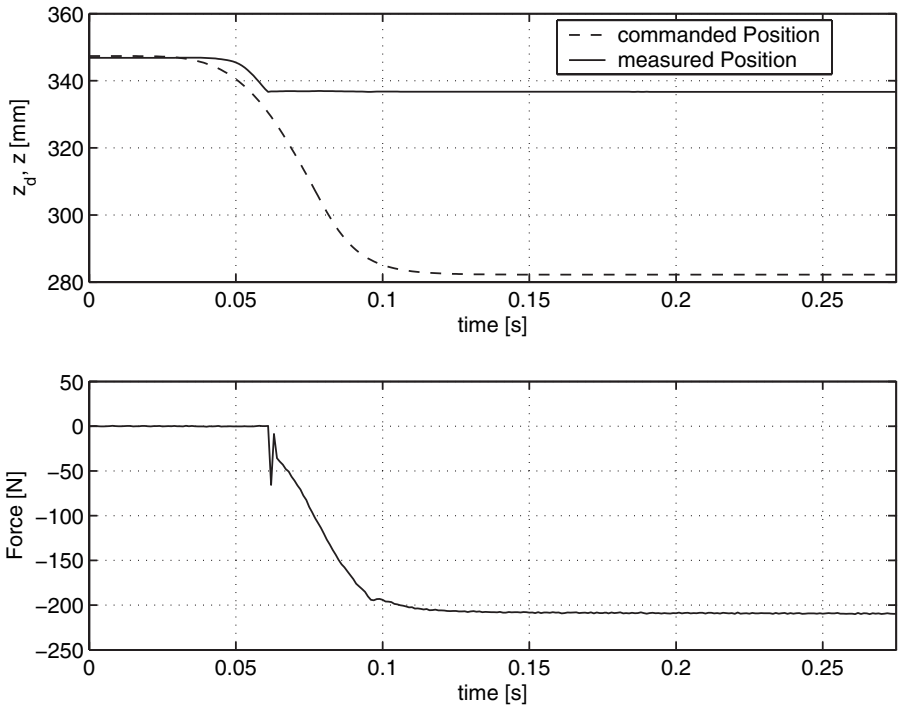

Fig. 6. The upper plot shows the desired and measured end-effector motion in the z-direction during the impact experiment. In the lower plot the contact force in the z-direction is displayed.

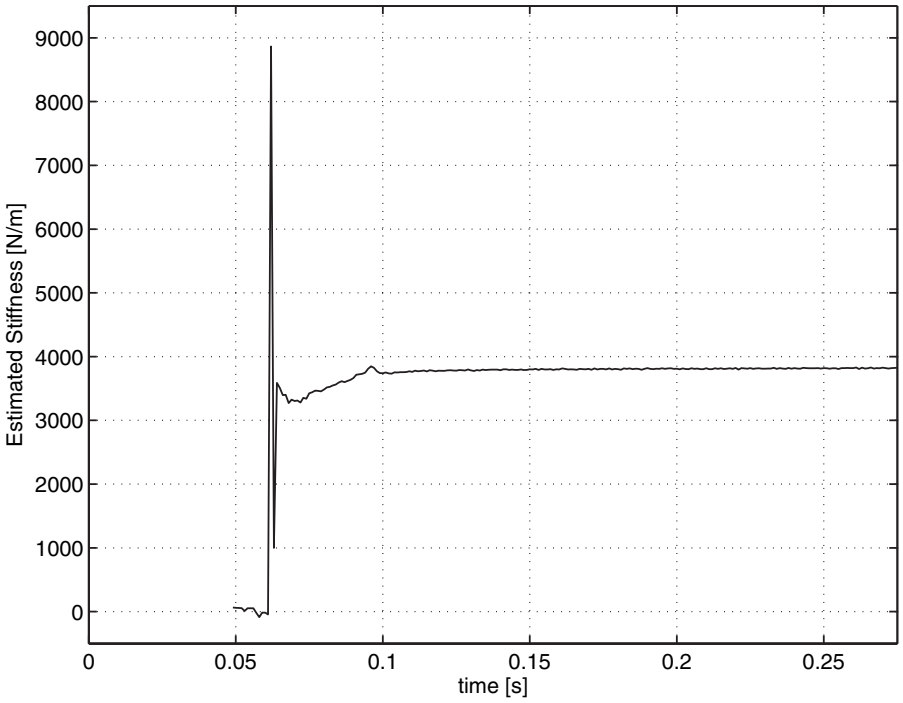

Fig. 7. Stiffness estimation during the impact experiment.

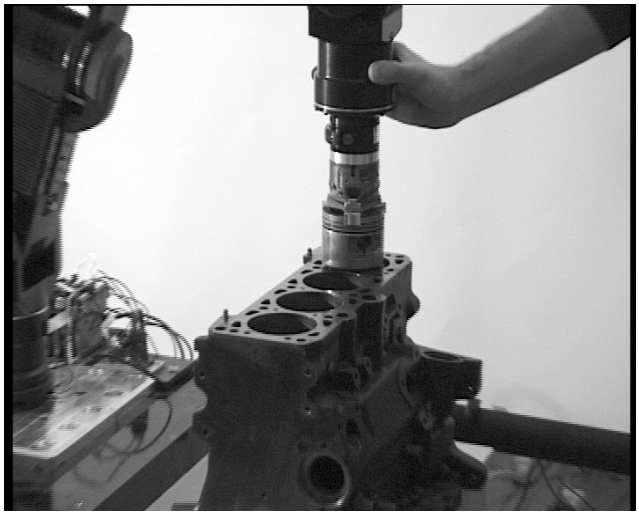

Fig. 8. Teaching phase for the automatic piston insertion using the lightweight robot II.

Fig. 9. Table wiping with null space movement.

piston insertion. The whole task was split into similar guiding and impedance control phases as in the piston insertion application. Figure 9 and Extension 2 show a demonstration at the Hannover fair in which the robot's elbow is deflected within its null space. Using the Cartesian controller, the robot continues wiping the table and applying a constant force in the vertical direction while for the redundant null space motion the robot has zero stiffness. For these experiments the Cartesian stiffness matrix was chosen as a diagonal matrix $\boldsymbol{K}_x = \text{diag}[k_t, k_t, 0, k_r, k_r, k_r]$ with $k_t = 2000$ N/m for the translational part and $k_r = 100$ Nm/rad for the rotational part. The stiffness value corresponding to the vertical motion was set to zero, and a constant vertical force of -10 N was added to the Cartesian command instead in order to keep contact with the table.

Opening a Door

In another service robotics application we used the Cartesian impedance control of the DLR lightweight robot II in order to open a door. Here the arm was used in combination with a mobile platform and the DLR hand II, Figure 10, Extension 3.

In this application, first, the door handle was manipulated by a sequence of impedance controlled movements in order to open the door. During these motions the measurements of the joint torques provided an estimate of the contact force and thus of the current contact state.

When the mobile platform finally moved through the door hinge, the door was kept at a distance by impedance control of the arm. Therefore, instead of using the stiffness term from Section 4.1, in this stage the desired impedance was based on an appropriate potential function, which has its minimum

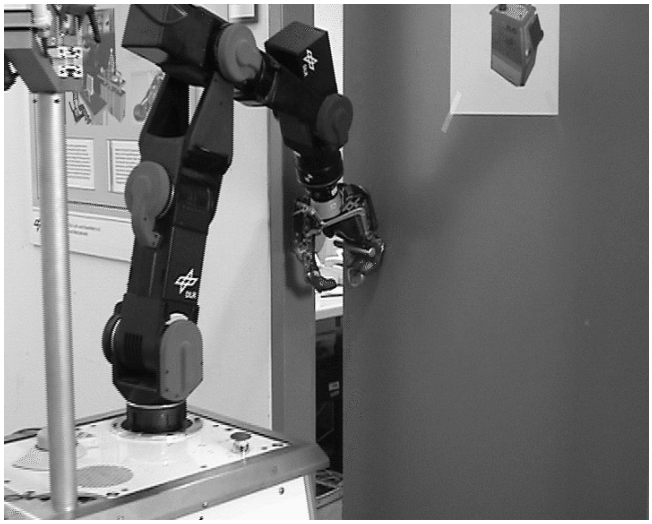

Fig. 10. DLR lightweight robot II while opening a door.

along a circularly shaped path with respect to a platform fixed frame. Additionally, the rotational stiffness was set to zero such that the end-effector orientation automatically adjusted.

7. Conclusions

In this paper, a unified, passivity-based perspective was given to the problem of position, torque and impedance control of flexible joint robots, at both joint and Cartesian level. These methods are especially relevant for lightweight, compliant robots designed for service applications or for human–robot

interaction. A physical interpretation was given for the torque controller and an energy shaping method was designed, which is based only on motor position (collocated controller), but which satisfies the static requirements formulated in terms of the robot end-effector. It is worth noting that the proposed energy shaping method can be generalized to a broader class of underactuated Euler–Lagrange systems (Albu-Schäffer et al. 2005), namely to systems that can be stabilized by shaping the potential energy only. An important advantage of these passivity-based controllers is the robustness with respect to uncertainties of the robot or load parameters, as well as to contact situations with unknown but passive environments. These properties were validated during numerous applications with the DLR lightweight robots, the newest one involving a humanoid upper body system (Extension 4), as well as crash test experiments for safety validation (Extension 5).

Appendix A

The well known stability analysis for PD control and gravity compensation of flexible joint robots (Tomei 1991) directly applies also to the case of the controller given by (6), (10). The analysis is given in a new, more general form, which allows a direct generalization to a wider class of Euler–Lagrange systems with less control inputs than states. It was shown in Section 3.2 that the effect of the torque controller is to reduce the motor inertia and that the dynamics of the torque controlled robot can be written as

$$\boldsymbol{M}(\boldsymbol{q})\ddot{\boldsymbol{q}} + \boldsymbol{C}(\boldsymbol{q},\dot{\boldsymbol{q}})\dot{\boldsymbol{q}} + \boldsymbol{g}(\boldsymbol{q}) = \boldsymbol{\tau} + \boldsymbol{D}\boldsymbol{K}^{-1}\dot{\boldsymbol{\tau}} + \boldsymbol{\tau}_{\text{ext}} \tag{42}$$

$$\boldsymbol{B}_\theta\ddot{\boldsymbol{\theta}} + \boldsymbol{\tau} + \boldsymbol{D}\boldsymbol{K}^{-1}\dot{\boldsymbol{\tau}} = \boldsymbol{u}. \tag{43}$$

By using the relation (5), the controller can be written as

$$\boldsymbol{u} = -\boldsymbol{K}_\theta\tilde{\boldsymbol{\theta}} - \boldsymbol{D}_\theta\dot{\boldsymbol{\theta}} + \boldsymbol{K}(\boldsymbol{\theta}_d - \boldsymbol{q}_d). \tag{44}$$

Therefore the system is equivalent to a flexible joint robot having the inertia $\boldsymbol{B}_\theta$ and controlled with a PD controller with gravity compensation. The equilibrium equations corresponding to (42), (43) for $\boldsymbol{\tau}_{\text{ext}} = \boldsymbol{0}$ are related to the minima of the potential energy $U(\boldsymbol{\theta},\boldsymbol{q}) = \frac{1}{2}(\boldsymbol{\theta}-\boldsymbol{q})^T\boldsymbol{K}(\boldsymbol{\theta}-\boldsymbol{q}) + V_g(\boldsymbol{q})$:

$$\frac{\partial U(\boldsymbol{\theta},\boldsymbol{q})}{\partial\boldsymbol{\theta}} = \boldsymbol{u} \tag{45}$$

$$\frac{\partial U(\boldsymbol{\theta},\boldsymbol{q})}{\partial\boldsymbol{q}} = \boldsymbol{0}. \tag{46}$$

First, notice that the desired motor position $\boldsymbol{\theta}_d$ corresponding to a desired link side position $\boldsymbol{q}_d$ has to satisfy (46), i.e., $\frac{\partial U(\boldsymbol{\theta}_d,\boldsymbol{q}_d)}{\partial\boldsymbol{q}} = \boldsymbol{0}$. This equation can be directly solved for $\boldsymbol{\theta}_d$, leading to (5). Second, notice that the static part of the controller (44) can be written as

$$\boldsymbol{u} = \frac{\partial U(\boldsymbol{\theta}_d,\boldsymbol{q}_d)}{\partial\boldsymbol{\theta}} + \frac{\partial U_s(\tilde{\boldsymbol{\theta}})}{\partial\boldsymbol{\theta}}, \tag{47}$$

where the first term is compensating for the left side of (45) at the desired position, while $U_s(\tilde{\boldsymbol{\theta}}) = \frac{1}{2}\tilde{\boldsymbol{\theta}}^T\boldsymbol{K}_\theta\tilde{\boldsymbol{\theta}}$ is the potential of the joint controller "spring" and is zero for $\boldsymbol{\theta} = \boldsymbol{\theta}_d$. By using the further notation $U_P(\boldsymbol{w}) = U(\boldsymbol{w}) + U_s(\boldsymbol{\theta})$ with $\boldsymbol{w} = (\boldsymbol{\theta},\boldsymbol{q})$, the equilibrium equations of the controlled robot can be written in the simple form

$$\frac{\partial U_P(\boldsymbol{w})}{\partial\boldsymbol{w}} - \frac{\partial U_P(\boldsymbol{w}_d)}{\partial\boldsymbol{w}} = \boldsymbol{0}. \tag{48}$$

Now consider finally the function

$$V_P(\boldsymbol{w}) = U_P(\boldsymbol{w}) - U_P(\boldsymbol{w}_d) - \frac{\partial U_P(\boldsymbol{w}_d)}{\partial\boldsymbol{w}}(\boldsymbol{w}-\boldsymbol{w}_d) \tag{49}$$

and notice that with this function, the stationary points of the system satisfy simply

$$\frac{\partial V_P(\boldsymbol{w})}{\partial\boldsymbol{w}} = \boldsymbol{0}. \tag{50}$$

It is directly verified that $V_P(\boldsymbol{w}_d) = 0$ holds and also that the point $\boldsymbol{w} = \boldsymbol{w}_d$ is an extremal point of $V_P(\boldsymbol{w})$ due to $\frac{\partial V_P(\boldsymbol{w}_d)}{\partial\boldsymbol{w}} = \boldsymbol{0}$ and therefore satisfies the system equilibrium equations. If the Hessian of $V_P(\boldsymbol{w})$, given by

$$\frac{\partial^2 V_P(\boldsymbol{w})}{\partial\boldsymbol{w}^2} = \begin{bmatrix} \boldsymbol{K}+\boldsymbol{K}_\theta & -\boldsymbol{K} \\ -\boldsymbol{K} & \boldsymbol{K} + \frac{\partial\boldsymbol{g}(\boldsymbol{q})}{\partial\boldsymbol{q}} \end{bmatrix} \tag{51}$$

is positive definite, then $\boldsymbol{w}_d$ is the only equilibrium point. This can always be satisfied for high enough gains $\boldsymbol{K}_\theta$ if the lower-right sub-matrix is positive definite, implying that the robot is stiff enough to sustain its own weight in the gravity field. Then, by adding the pseudo[14] kinetic energy $T_\theta(\boldsymbol{w},\dot{\boldsymbol{w}}) = \frac{1}{2}(\dot{\boldsymbol{q}}^T\boldsymbol{M}(\boldsymbol{q})\dot{\boldsymbol{q}} + \dot{\boldsymbol{\theta}}^T\boldsymbol{B}_\theta\dot{\boldsymbol{\theta}})$, one obtains a candidate Lyapunov function

$$V(\boldsymbol{w},\dot{\boldsymbol{w}}) = T(\boldsymbol{w},\dot{\boldsymbol{w}}) + V_P(\boldsymbol{w}), \tag{52}$$

which is clearly positive definite and radially unbounded. Since, after some direct calculations one obtains

$$\dot{V}(\dot{\boldsymbol{w}}) = -\dot{\boldsymbol{\theta}}^T\boldsymbol{D}_\theta\dot{\boldsymbol{\theta}} - (\dot{\boldsymbol{\theta}}-\dot{\boldsymbol{q}})^T\boldsymbol{D}(\dot{\boldsymbol{\theta}}-\dot{\boldsymbol{q}}), \tag{53}$$

which is always negative definite in $\dot{\boldsymbol{w}}$, asymptotic stability can be shown using LaSalle's invariance principle.

If one considers the controller (8) and hence the controlled motor dynamics (9) instead of (43) the same Lyapunov function (52) has time derivative given by

$$\dot{V}_1(\dot{\boldsymbol{w}}) = -\dot{\boldsymbol{\theta}}^T\boldsymbol{D}_\theta\dot{\boldsymbol{\theta}} - (\dot{\boldsymbol{\theta}}-\dot{\boldsymbol{q}})^T\boldsymbol{D}(\dot{\boldsymbol{\theta}}-\dot{\boldsymbol{q}}) + \dot{\boldsymbol{\theta}}^T(\boldsymbol{D}-\boldsymbol{D}_s)(\dot{\boldsymbol{\theta}}-\dot{\boldsymbol{q}}). \tag{54}$$

This time derivative is negative definite if the following condition is fulfilled

$$\boldsymbol{D} > \frac{1}{4}(\boldsymbol{D}-\boldsymbol{D}_s)^T\boldsymbol{D}_\theta(\boldsymbol{D}-\boldsymbol{D}_s). \tag{55}$$

14. $\boldsymbol{B}_\theta$ is used instead of $\boldsymbol{B}$.

REMARK 3. Notice that the control law (47) and the potential function (49) can be extended to a more general class of underactuated systems, for which there exists a one to one relation between the directly actuated configuration variables $\boldsymbol{\theta}$ and the indirectly actuated configurations $\boldsymbol{q}$.

Appendix B: Index to Multimedia Extensions

The multimedia extension page is found at http://www.ijrr.org.

Table of Multimedia Extensions

Extension	Type	Description
1	Video	Cartesian impedance control is used for teaching and execution of piston insertion. For comparison, the human execution is shown.
2	Video	Table wiping with simultaneous null-space movement and force control in vertical direction.
3	Video	Door opening using impedance control.
4	Video	Position control of the new humanoid system Justin.
5	Video	Crash test experiments for safety validation[1]

[1]These experiments were done together with Sami Haddadin. A paper describing the experiments is currently in preparation.

References

Albu-Schäffer, A. (2002). *Regelung von Robotern mit elastischen Gelenken am Beispiel der DLR-Leichtbauarme*. PhD thesis, Technical University Munich, April.

Albu-Schäffer, A. and Hirzinger, G. (2001). A globally stable state-feedback controller for flexible joint robots. *Journal of Advanced Robotics, (Special Issue: Selected Papers from IROS 2000)* **15**(8): 799–814.

Albu-Schäffer, A., Ott, C., Frese, U., and Hirzinger, G. (2003). Cartesian impedance control of redundant robots: Recent results with the dlr-light-weight-arms. *IEEE International Conference on Robotics and Automation*, pp. 3704–3709.

Albu-Schäffer, A., Ott, C. and Hirzinger, G. (2004a). Passivity based cartesian impedance control for flexible joint manipulators. *6th IFAC Symposium on Nonlinear Control Systems*, Vol. 2, pp. 1175–1180.

Albu-Schäffer, A., Ott, C., and Hirzinger, G. (2004b). A passivity based cartesian impedance controller for flexible joint robots—Part II: Full state feedback, impedance design and experiments. *IEEE International Conference on Robotics and Automation*, pp. 2666–2673.

Albu-Schäffer, A., Ott, C., and Hirzinger, G. (2005). Constructive energy shaping based impedance control for a class of underactuated Euler-Lagrange systems. *IEEE International Conference on Robotics and Automation*, pp. 1399–1405.

Bicchi, A., Tonietti, G., Bavaro, M., and Piccigallo, M. (2003). Variable stiffness actuators for fast and safe motion control. *IEEE International Symposium on Robotics Research*.

Brogliato, B., Ortega, R., and Lozano, R. (1995). Global tracking controllers for flexible-joint manipulators: a comparative study. *Automatica* **31**(7): 941–956.

Burdick, J. (1995). A classification of 3R regional manipulator singularities and geometries. *Mechanism and Machine Theory* **30**(1): 71–89.

Chen, S. and Kao, I. (2000). Simulation of conservative congruence transformation conservative properties in the joint and Cartesian spaces. *IEEE International Conference on Robotics and Automation*, pp. 1283–1288.

Goldsmith, P. B., Francis, B. A., and Goldenberg, A. A. (1999). Stability of hybrid position/force control applied to manipulators with flexible joints. *International Journal of Robotics and Automation* **14**(4): 146–159.

Hirzinger, G., Albu-Schäffer, A., Hähnle, M., Schaefer, I., and Sporer, N. (2001). On a new generation of torque controlled light-weight robots. *IEEE International Conference on Robotics and Automation*, pp. 3356–3363.

Hogan, N. (1985). Impedance control: An approach to manipulation, Part I—Theory, Part II—Implementation, Part III—Applications. *ASME Journal of Dynamic Systems, Measurement and Control* **107**: 1–24.

Kelly, R. (1997). PD control with desired gravity compensation of robotic manipulators: A review. *International Journal of Robotics Research* **16**(5): 660–672.

Kelly, R. and Santibanez, V. (1998). Global regulation of elastic joint robots based on energy shaping. *IEEE Transactions on Automatic Control* **43**(10): 1451–1456.

Khatib, O. (1995). Inertial properties in robotic manipulation: An object level framework. *International Journal of Robotics Research* **14**(1): 19–36.

Lin, T. and Goldenberg, A. A. (1995). Robust adaptive control of flexible joint robots with joint torque feedback. *IEEE International Conference on Robotics and Automation*, pp. 1229–1234.

Lozano, R., Brogliato, B., Egeland, O., and Maschke, B. (2000). *Dissipative Systems Design and Control*. Comunication and Control Engineering. Springer.

De Luca, A. (2000). Feedforward/feedback laws for the control of flexible robots. *IEEE International Conference on Robotics and Automation*, pp. 233–240.

De Luca, A. and Lucibello, P. (1998). A general algorithm for dynamic feedback linearization of robots with

elastic joints. *IEEE International Conference on Robotics and Automation*, pp. 504–510.

Lückel, J., Moritz, W., Neumann, R., Schütte, H., and Wittler, G. (1993). Development of a modular mechatronic robot system. *2nd Conference on Mechatronics and Robotics*.

Morita, T., Iwata, H., and Sugano, S. (1999). Development of human symbiotic robot: Wendy. *IEEE International Conference on Robotics and Automation*, pp. 3183–3188.

Nicosia, S. and Tomei, P. (1992). A method to design adaptive controllers for flexible joint robots. *IEEE International Conference on Robotics and Automation*, pp. 701–706.

Ortega, R., Kelly, R., and Loria, A. (1995). A class of output feedback globally stabilizing controllers for flexible joint robots. *IEEE International Journal of Robotics and Automation* **11**(5): 766–770.

Ott, C., Albu-Schäffer, A., and Hirzinger, G. (2002). Comparison of adaptive and nonadaptive tracking control laws for a flexible joint manipulator. *IEEE International Conference on Intelligent Robotic Systems*, pp. 2018–2024.

Ott, C., Albu-Schäffer, A., and Hirzinger, G. (2004). A passivity based cartesian impedance controller for flexible joint robots—Part I: Torque feedback and gravity compensation. *IEEE International Conference on Robotics and Automation*, pp. 2659–2665.

Pratt, G. A. and Williamson, M. (1995). Series elastics actuators. *Proceedings of IEEE/RSJ International Conference on Intelligent Robots and Systems*, pp. 399–406.

Spong, M. (1987). Modeling and control of elastic joint robots. *ASME Journal of Dynamic Systems, Measurement, and Control* **109**: 310–319.

Spong, M. (1989). Adaptive control of flexible joint manipulators. *Systems and Control Letters* **13**: 15–21.

Spong, M. (1995). Adaptive control of flexible joint manipulators: Comments on two papers. *Automatica* **31**(4): 585–590.

Stelter, J. (2001). *Verbesserung des Positionsverhaltens und der Bahntreue eines Industrieroboters durch Einsatz von Beschleunigungssensoren*. PhD thesis, Fakultät für Informatik der University Karlsruhe.

Takegaki, M. and Arimoto, S. (1981). A new feedback method for dynamic control of manipulators. *ASME Journal on Dynamic Systems, Measurement and Control* **102**: 119–125.

Tomei, P. (1991). A simple PD controller for robots with elastic joints. *IEEE Transactions on Automatic Control* **36**(10): 1208–1213.

Vidyasagar, M. (1978). *Nonlinear Systems Analysis*. Prentice-Hall.

Wenger, P. (1998). Classification of 3R positioning manipulators. *ASME Journal of Mechanical Design* **120**(2): 327–332.

Yim, W. (2001). Adaptive control of a flexible joint manipulator. *IEEE International Conference on Robotics and Automation*, pp. 3441–3446.

Zhu, W. and De Schutter, J. (1999). Adaptive control of mixed rigid/flexible joint robot manipulators based on virtual decomposition. *IEEE Transactions on Robotics and Automation* **15**(2): 310–317.

Zinn, M., Khatib, O., and Roth, B. (2004). A new actuation approach for human friendly robot design. *International Journal of Robotics Research* **23**: 279–398.

Zollo, L., Siciliano, B., De Luca, A., Guglielmelli, E., and Dario, P. (2005). Compliance control for an anthropomorphic robot with elastic joints: Theory and experiments. *ASME Journal of Dynamic Systems, Measurements and Control* **127**(3): 321–328.